# Computing photoionization spectra in Gaussian basis sets

Ivan Duchemin, Antoine Levitt

# Computing photoionization spectra in Gaussian basis sets

Ivan Duchemin[*], Antoine Levitt[†]

**Abstract**

We present a method to compute the photoionization spectra of atoms and molecules in linear response time-dependent density functional theory. The electronic orbital variations corresponding to ionized electrons are expanded on a basis set of delocalized functions obtained as the solution of the inhomogeneous Helmholtz equation with gaussian basis set functions as right-hand side. The resulting scheme is able to reproduce photoionization spectra without any need for artificial regularization or localization. We demonstrate that it is able to produce accurate spectra for semilocal exchange-correlation functionals even using relatively small standard gaussian basis sets.

## 1 Introduction

Time-dependent functional theory in the linear response regime (LR-TDDFT) is widely used to compute excitation energies of molecules. The traditional way to compute these properties involves solving the Casida equations [4], which are the discretized LR-TDDFT equations in a basis set of localized functions (typically, gaussian basis sets). This is very convenient for the excitations lying below the ionization potential, for which the orbital variations are localized functions. This however fails to reproduce the photoionization spectrum, turning a continuous function into a series of infinitely sharp peaks (Dirac deltas). These peaks approximate the function in a weak sense (when integrated against smooth functions) in the limit of complete basis sets [9], but pointwise values are not easily obtained.

Various techniques have been used to remedy this. The simplest and most general technique is to use an artificial dissipation parameter $\eta$. This effectively adds a constant imaginary part to the Hamiltonian, broadening the infinitely sharp peaks and producing a continuous function. Another related technique is the use of complex absorbing potentials, where the imaginary part is only made to act away from the molecule, effectively attempting to broaden only the states that correspond to ionized electrons [13]. Another variation on the same idea is to add the imaginary part to the molecular orbitals energies directly [6]. When implemented in the time domain, these techniques can be understood as adding an artificial dissipation, resulting in states with finite lifetimes (complex energies).

These schemes shift the poles of the response function away from the real axis into the lower complex plane, resulting in response functions that can mathematically be expressed as sums of Lorentzians. However, this does not respect the mathematical structure of photoionization spectra (infinitely sharp peaks before the ionization potential, continuous function with sharp changes around the ionization potentials as well as possible resonances). As a result, when the basis sets are small (as is the case for typical gaussian basis sets), spectra are often unsatisfactory.

Another class of methods attempts to recover the continuous photoionization spectrum from the discrete peaks by fitting rational functions to quantities that are computable on localized basis sets, such as moments of the oscillator strengths or values of the polarizability in the complex plane: examples include Stieljes imaging or Padé extrapolation (see [19] for a review). These methods are intrinsically numerically unstable and need a non-trivial manual parameter selection.

More sophisticated schemes like the complex scaling and exterior complex scaling methods use the analytic continuation of the solutions to transform oscillatory tails into decaying ones, resulting in more accurate

[*]Université Grenoble Alpes, CEA, IRIG-MEM-L Sim, 38054 Grenoble, France
[†]Université Paris-Saclay, CNRS, Laboratoire de mathématiques d'Orsay, 91405 Orsay, France

spectra [5]. These schemes are however non-trivial to implement, and require significant fine-tuning of parameters (as do the dissipation-based schemes).

A more principled class of methods involve solving an approximate form of the equation exactly outside of the computational domain, resulting in a Dirichlet-to-Neumann map that acts as an effective boundary condition [15]. These schemes are however hard to implement in systems without spherical symmetry.

In this paper, inspired by a method we recently developed to compute resonances in locally perturbed periodic media [7], we propose a new scheme that does not rely on artificial dissipation or localization methods, and works for arbitrary molecules without symmetries. The method can be summarized as follows. The LR-TDDFT equations for the orbital variations $\delta\psi_i^\pm$ are of the Helmholtz form

$$(\pm\omega + i0^+ + \varepsilon_i + \tfrac{1}{2}\Delta)\delta\psi_i^\pm = f$$

where $f$ is a localized function (that depends self-consistently on all the $\delta\psi_i^\pm$) and $\varepsilon_i < 0$ are the Kohn-Sham one-particle energies. The $i0^+$ in this equation means that the equation is to be solved for finite positive values $i\eta$, and $\eta$ is to be taken to tend to zero after the calculation.

From the form of the Green function of the operator $\pm\omega + i0^+ + \varepsilon_i + \frac{1}{2}\Delta$, it can be seen that, in the limit $\eta \to 0^+$, for $\omega > -\varepsilon_i$, $\delta\psi_i^+$ will be delocalized. Physically, $\delta\psi_i^+$ represents an electron ionization; the positive values of $\eta$ correspond to imposing an outgoing wave boundary condition. It is not appropriate to discretize the delocalized $\delta\psi_i^+$ on a localized basis set; in fact, doing so results in a singular photoionization limit that, in the limit $\eta \to 0^+$, tends to a finite sum of Dirac masses located at the Casida excitation energies. These then have to be regularized to obtain a continuous spectrum. Instead, we perform the change of variable

$$\delta\psi_i^+ = (\omega + i0^+ + \varepsilon_i + \tfrac{1}{2}\Delta)^{-1}\delta\phi_i^+,$$

and discretize $\phi_i^+$ (which is localized) on a standard gaussian basis set. Equivalently, we discretize $\delta\psi_i^+$ on a basis set consisting of solutions of the Helmholtz equation with gaussian basis set functions as right-hand side.

By respecting the structure of the equations (localized excitation or delocalized ionization, depending on the value of $\pm\omega + \varepsilon_i$), this method allows us to compute photoionization spectra directly. Compared to the standard method of solving the Casida equations, it is much more accurate, resulting in accurate spectra using very moderate basis sets. It can be easily adapted to compute resonances, and is fully general, being suited to molecules as well as atoms. The flip side is an added computational cost, which, although formally having the same cubic scaling as usual TDDFT methods, has a higher prefactor, mostly due to the need for frequency-dependent integrals on a real space grid. These are however highly parallelizable.

# 2 Methods

## 2.1 Model

We consider a molecule with $N$ spin-paired electrons modeled using time-dependent adiabatic Kohn-Sham density functional theory with a semilocal functional, and an electrostatic potential $V_{\text{nucl}}$ originating from the nuclei. The ground-state orbitals $\psi_i$ satisfy, for all $i \in \{1, \dots, N/2\}$,

$$H[\rho]\psi_i = \varepsilon_i\psi_i$$

where, in atomic units,

$$\begin{aligned} H[\rho] &= -\tfrac{1}{2}\Delta + V_{\text{tot}}[\rho] \\ V_{\text{tot}} &= V_{\text{nucl}} + V_{\text{Hxc}}[\rho] \\ V_{\text{Hxc}}[\rho](\mathbf{r}) &= \int \frac{\rho(\mathbf{r}')}{|\mathbf{r} - \mathbf{r}'|} d\mathbf{r}' + v_{\text{xc}}(\rho(\mathbf{r})) \end{aligned}$$

The total density is $\rho(\mathbf{r}) = 2\sum_{i=1}^{N/2} |\psi_i(\mathbf{r})|^2$. We choose the ground-state orbitals to be real for simplicity, but the scheme extends trivially to complex orbitals.

Consider now a perturbing potential $\delta V_{\mathcal{P}}$. In the time-harmonic regime, the first-order response can be described by the Sternheimer equations [15]

$$(\pm\omega + i\eta + \varepsilon_i - H[\rho])\delta\psi_i^{\pm} - (f_{\mathrm{HXC}}\delta\rho)\psi_i = \delta V_{\mathcal{P}}\psi_i$$

The variation in the Hartree-exchange-correlation kernel is given by

$$(f_{\mathrm{HXC}}\delta\rho)(\mathbf{r}) = \int \frac{\delta\rho(\mathbf{r}')}{|\mathbf{r}-\mathbf{r}'|}d\mathbf{r}' + v'_{\mathrm{xc}}(\rho(\mathbf{r}))\delta\rho(\mathbf{r}).$$

and the variation in density by

$$\delta\rho(\mathbf{r}) = 2\sum_{i=1}^{N/2} \psi_i(\mathbf{r})(\delta\psi_i^+(\mathbf{r}) + \delta\psi_i^-(\mathbf{r})).$$

This defines the total variation in polarization

$$\delta\mathbf{P} = \int \mathbf{r}\delta\rho(\mathbf{r})d\mathbf{r}.$$

When $\delta V_{\mathcal{P}}(\mathbf{r}) = -\mathbf{e}\cdot\mathbf{r}$, the linear relationship $\delta\mathbf{P} = \alpha(\omega+i\eta)\mathbf{e}$ defines the polarizability tensor $\alpha$, a $3\times 3$ matrix. Finally, the photoionization cross-section is given by

$$\sigma(\omega) = \lim_{\eta\to 0^+} \frac{4\pi\omega}{c}\frac{1}{3}\mathrm{Tr}(\alpha(\omega+i\eta)),$$

with $c$ the speed of light, and will be our main observable of interest.

## 2.2 Integral form and delocalization

The standard approach to discretizing these equations is to expand $\delta\psi_i$ in a basis, which leads to the usual Casida equations. This is however inefficient when $\omega$ is greater than $-\varepsilon_i$, at which point the electron becomes ionized and $\delta\psi_i^+$ is delocalized. To see this, we write the Sternheimer equations as

$$(\pm\omega + i\eta + \varepsilon_i + \tfrac{1}{2}\Delta)\delta\psi_i^{\pm} = V_{\mathrm{tot}}\delta\psi_i^{\pm} + (f_{\mathrm{HXC}}\delta\rho)\psi_i + \delta V_{\mathcal{P}}\psi_i \tag{1}$$

Since $V_{\mathrm{tot}}$ and $\psi_i$ are localized, the right-hand side is localized. Introduce the free Green's function $G_0(\mathbf{r},\mathbf{r}';z)$, the kernel of the inverse of the operator $z+\frac{1}{2}\Delta$, well-defined when $\eta>0$. We can then reformulate the Sternheimer equations in integral form

$$\delta\psi_i^{\pm} = G_0(\pm\omega+i\eta+\varepsilon_i)\Big(V_{\mathrm{tot}}\delta\psi_i^{\pm} + (f_{\mathrm{HXC}}\delta\rho)\psi_i + \delta V_{\mathcal{P}}\psi_i\Big)$$

An explicit computation shows that the kernel of the Green function is given by

$$G_0(\mathbf{r},\mathbf{r}',z) = -\frac{1}{2\pi}\frac{e^{ik(z)|\mathbf{r}-\mathbf{r}'|}}{|\mathbf{r}-\mathbf{r}'|}$$

where $k(z)$ is the square root of $2z$ with positive imaginary part (so that $G_0$ is localized when $\eta>0$).

When $z = \pm\omega + i\eta + \varepsilon_i$ approaches the real axis, this Green function is oscillatory when $\mathrm{Re}(z)>0$, and decaying when $\mathrm{Re}(z)<0$. In the region $\omega>0$, $-\omega+\varepsilon_i$ is always negative, and therefore $\delta\psi_i^-$ will be localized. However, the behavior of $\psi_i^+$ depends on whether $\omega<-\varepsilon_i$ or $\omega>\varepsilon_i$ (below or above ionization threshold). In the case $\omega<-\varepsilon_i$, $\delta\psi_i^+$ will be localized; in the case $\omega<-\varepsilon_i$, it will be oscillatory. This explains why usual methods, based on the discretization of $\delta\psi_i$, have trouble reproducing the ionization region $\omega>-\varepsilon_i$.

## 2.3 Our method

Our approach is to use the change of variables

$$\delta\psi_i^+ = G_0(\pm\omega + i\eta + \varepsilon_i)\delta\phi_i^+ \text{ when } \omega + \varepsilon_i > 0$$

and to discretize $\delta\phi_i^+$ in a Gaussian basis set instead of $\delta\psi_i^+$ directly. This ensures automatically the correct asymptotic behavior for $\delta\psi_i^+$. The $\delta\phi_i^+$ satisfy the integral equation

$$\delta\phi_i^+ - V_{\text{tot}}G_0(+\omega + i\eta + \varepsilon_i)\delta\phi_i^+ - (f_{\text{HXC}}\delta\rho)\psi_i = \delta V_{\mathcal{P}}\psi_i \tag{2}$$

When $\pm\omega + \varepsilon_i \leq 0$, we discretize $\delta\psi_i^\pm$ in the usual way on a basis of Gaussian-type orbitals $(\chi_\alpha)_{\alpha=1,\ldots,N_b}$. When $\pm\omega + \varepsilon_i > 0$, we discretize $\delta\phi_i^\pm$ on the basis:

$$\delta\phi_i^+(\mathbf{r}) = \sum_{\alpha=1}^{N_b} a_{i\alpha}^+\chi_\alpha(\mathbf{r}) \text{ when } \omega + \varepsilon_i > 0$$
$$\delta\psi_i^\pm(\mathbf{r}) = \sum_{\alpha=1}^{N_b} b_{i\alpha}^\pm\chi_\alpha(\mathbf{r}) \text{ otherwise}$$

This sets up a linear system in the coefficients $(a, b)$.

Note that from (2) it follows that $\delta\phi_i^+$ is as localized as $V_{\text{tot}}\psi_i^+$. Therefore, the decay of the total mean-field potential determines the localization of $\delta\phi_i^+$, and therefore the effectiveness of the numerical method. When using semilocal density functionals (with exponentially decaying exchange-correlation potentials), this is determined by the electrostatic potential. We can therefore rank systems by decreasing order of localization: atoms (exponentially decaying potential), nonpolar molecules (potential decaying as $1/r^3$), polar molecules ($1/r^2$), charged systems ($1/r$). When using hybrid functionals incorporing Hartree-Fock exchange, the effective potential seen by ionized electrons behaves as $1/r$ [15], and we expect our method to have difficulties.

## 2.4 Solution of the linear system

We project the Sternheimer equations (1) and (2) on the basis to obtain

$$\begin{cases} (S - K_i^+)a_i^+ - g_i[a,b] = h_i & \text{when } \omega + \varepsilon_i > 0 \\ ((\pm\omega + \varepsilon_i + i\eta)S - H)b_i^\pm - g_i[a,b] = h_i & \text{otherwise,} \end{cases} \tag{3}$$

where

$$\begin{aligned} S_{\alpha\beta} &= \langle\chi_\alpha|\chi_\beta\rangle \\ H_{\alpha\beta} &= \langle\chi_\alpha| - \tfrac{1}{2}\Delta + V_{\text{tot}}|\chi_\beta\rangle \\ K_{i\alpha\beta}^+ &= \langle\chi_\alpha|V_{\text{tot}}G_0(+\omega + i\eta + \varepsilon_i)|\chi_\beta\rangle \\ g_{i\alpha}[a,b] &= \langle\chi_\alpha|f_{\text{HXC}}\delta\rho[a,b]|\psi_i\rangle \\ h_{i\alpha} &= \langle\chi_\alpha|\delta V_{\mathcal{P}}|\psi_i\rangle \end{aligned}$$

The computation of $S$, $H$ and $h_i$ are standard. For $K$, the matrix elements are not analytic. However, the values $(G_0(\pm\omega + i\eta + \varepsilon_i)\chi_\beta)(\mathbf{r})$ can be computed analytically for all $\mathbf{r}$ (see Appendix). Therefore, we introduce an integration grid with points $\mathbf{r}_l$ and weights $w_l$, and approximate $K_{\alpha\beta}$ as

$$K_{\alpha\beta} \approx \sum_l w_l\chi_\alpha(\mathbf{r}_l)V_{\text{tot}}(\mathbf{r}_l)(G_0(\pm\omega + i\eta + \varepsilon_i)\chi_\beta)(\mathbf{r}_l).$$

The values of $V_{\text{tot}}(\mathbf{r}_l)$ arising from the nuclei and exchange-correlation terms are computed exactly, as is usual in DFT. Note that since the delocalizing operator $G_0$ is then multiplied by localized quantities, the grid only needs to be sufficient to integrated localized functions. In practice, we found that a coarse exchange-correlation grid was often adequate.

The computation of $g$, assuming that all the $(a, b)$ are known, is more conveniently reformulated as

$$g_{i\alpha} = \langle \delta\rho[a, b] | f_{\text{HXC}} \psi_i \chi_\alpha \rangle.$$

The values of $f_{\text{HXC}}\psi_i\chi_\alpha$ on the grid are precomputed, using the same technique as for the computation of $V_{\text{tot}}$. Then, $\delta\rho[a, b](\mathbf{r}) = 2\sum_{j=1}^{N/2} \psi_j(\mathbf{r})(\delta\psi_j^+(\mathbf{r}) + \delta\psi_j^-(\mathbf{r}))$ is formed on the grid, by using the values of $G_0(\pm\omega + i\eta + \varepsilon_i)\chi_\alpha$ on the grid and the $(a, b)$ coefficients.

The linear system (3) is solved with the GMRES iterative solver, preconditioned by $S - K_i^+$ (for the $a$ block) and $(\pm\omega + \varepsilon_i)S - H$ (for the $b$ block).

The additional computational cost compared to standard iterative TDDFT computations is summarized in Table 1. Note that these steps are cubic scaling (and, for low-lying excitations where the number of ionized electrons is of the order of unity, quadratically scaling) except for the steps involving $f_{\text{HXC}}$. The scaling can be improved using techniques such as the resolution of the identity. However, in our tests, the step involving the computation of the values of $G_0\chi_\alpha$ on the grid dominated the overall computational time, and therefore we did not optimize the other steps.

| Operation | Cost |
|---|---|
| Precomputations of $f_{\text{HXC}}\psi_i\chi_\alpha$ | $N_{\text{g}}N_{\text{occ}}N_{\text{b}} + N_{\text{b}}^2 N_{\text{g}}N_{\text{occ}}$ |
| Computation of $G_0(\pm\omega + i\eta + \varepsilon_i)\chi_\alpha$ on the grid | $N_\omega N_{\text{ionized}} N_{\text{g}} N_{\text{b}}$ |
| Matrix-vector products with $K$ | $N_\omega N_{\text{ionized}} N_{\text{iter}} N_{\text{g}} N_{\text{b}}$ |

Table 1: Dominant scaling of the main operations compared to standard iterative TDDFT. $N_{\text{b}}$ is the number of basis functions, $N_{\text{g}}$ the number of grid points, $N_{\text{occ}}$ the number of occupied orbitals, $N_{\text{ionized}}$ the number of ionized orbitals. Typically, $N_{\text{ionized}} \ll N_{\text{occ}} \ll N_{\text{b}} \ll N_{\text{g}}$. Additionally, $N_\omega$ is the number of frequencies desired, and $N_{\text{iter}}$ is the number of iterations of the iterative solver (typically, $\leq 10$).

# 3 Results

We implemented the method in the Julia programming language [3], interfacing with the PySCF package [16] to perform the initial setup and DFT run. The integrals described in the Appendix were implemented in the GaIn Fortran library. The code is freely available at `https://github.com/antoine-levitt/PhotoionizationGTO.jl` and `https://gitlab.maisondelasimulation.fr/beDeft/GaIn`.

All results presented below use the LDA exchange-correlation functional, with no spin polarization. The use of the LDA functional is inadequate to obtain accurate photoionization spectra for the systems studied here, but the emphasis in this paper is on the methodology rather than on the particular results.

Unless explicitly mentioned, we used a very coarse exchange-correlation grid (PySCF setting `1`), which yielded reasonably accurate results at minimal computational cost. We used the Dunning augmented basis sets [8, 11], as provided by the basis set exchange [14]. These basis sets are designed for converging post-Hartree-Fock methods rather than TDDFT properties, and are very suboptimal here. We simply use them to demonstrate that acceptable convergence can be obtained in basis sets not specifically designed for that purpose.

## 3.1 Atoms

Atoms have an exponentially decaying total potential; therefore, we expect the $\delta\phi$ to be exponentially localized, making it an ideal case for our method. On atoms, we are able to compare the results to a

reference (black line) computed using the atom-specific method of [15]. We focus in this section on He and Be atoms.

Helium is the simplest system, with only one occupied orbital (1s). Accordingly, its TDLDA photoionization spectrum has only one threshold, plotted as a dashed vertical line. We see that results are already

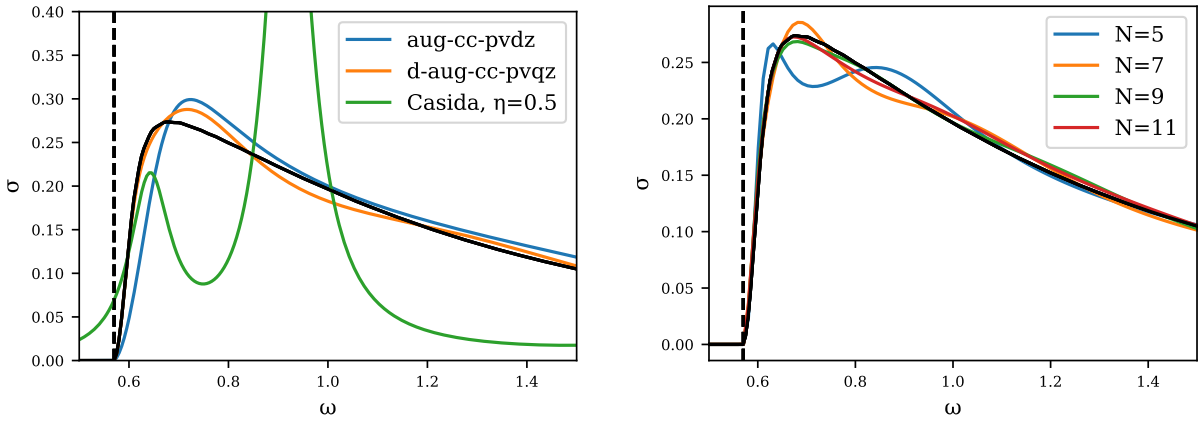


Figure 1: Photoionization of Helium, with standard basis sets (left) and even-tempered basis sets (right). The result of the standard Casida method with damping ($\eta = 0.5$) in the d-aug-cc-pvqz basis set is shown for comparison. Reference data (black line) from the method of [15].

qualitatively consistent even at extremely coarse basis sets: note for instance that the basis set aug-cc-pvdz only has two basis functions for the p channel relevant here. To check systematic convergence, we used a basis of even-tempered gaussians with $N$ gaussian exponents logarithmically spaced from 0.01 to 10 (these values are taken somewhat arbitrarily and not optimized).

To appreciate how inadequate the Casida method is to compute photoionization spectra on this system, note that, in the largest basis set used here, d-aug-cc-pvqz and in the frequency range displayed here, there are only two relevant (1s $\to$ 2p) excitations, at $\omega = 0.64$ and $\omega = 0.91$. This is clearly not sufficient to reconstruct a full spectrum. The same goes for other approaches such as complex absorbing potentials; these methods, even with optimal parameters, will only move these two poles in the complex plane, which is not sufficient to reproduce the full structure of the spectrum.

To illustrate, we plot Figure 2 for $\omega = 1$ the orbital variation $\delta\psi^+$, as well as the localized $\delta\phi^+$ defined by $\delta\psi^+ = G_0(\omega + i0^+)\delta\phi^+$. It is clearly not possible to represent the delocalized variation $\delta\psi^+$ by localized orbitals, but $\delta\phi^+$ is relatively short-range and therefore can reasonably be expanded on a gaussian basis set.

Beryllium has two occupied orbitals (1s and 2s), yielding two different thresholds. Here, small standard basis sets are inaccurate, showing a displaced peak after the $2s$ ionization and unphysical oscillations after the $1s$ ionization. Using even-tempered basis set (using 10 gaussians with exponents logarithmically spaced between 0.01 and 10) yields an almost perfect ionization spectrum.

The ionization threshold of the 2s orbital lies below the 1s$\to$2p excitation energy, which turns into a resonance. This resonance, extremely hard to capture with standard damping methods, is present and relatively accurate even with very coarse basis sets. Note that, since we are able to compute analytic continuations of the matrix elements of the free Green function as $z$ crosses the positive real axis, we could compute this resonance directly [7], but we do not pursue this direction in this paper.

## 3.2 Nonpolar molecules

We next try our method on nonpolar molecules, on which the asymptotic decay of the total potential is dictated by the quadrupole moment (decaying thus as $1/r^3$). The test was conducted for $H_2$ and $CH_4$, demonstrating a rapid convergence with respect to the basis set used: in both cases the spectrum is already

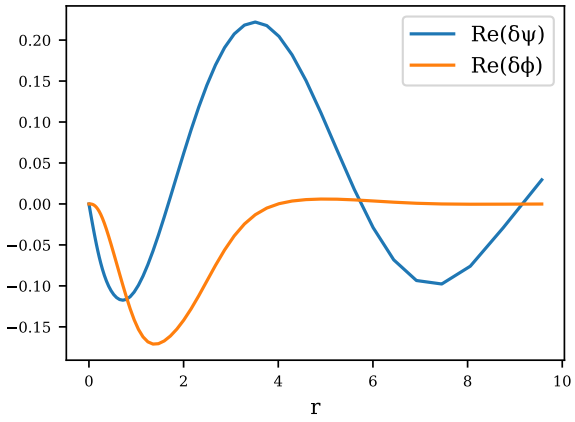


Figure 2: Orbital variations $\delta\psi^+$ and $\delta\phi^+$ (see text) for Helium at $\omega = 1$.

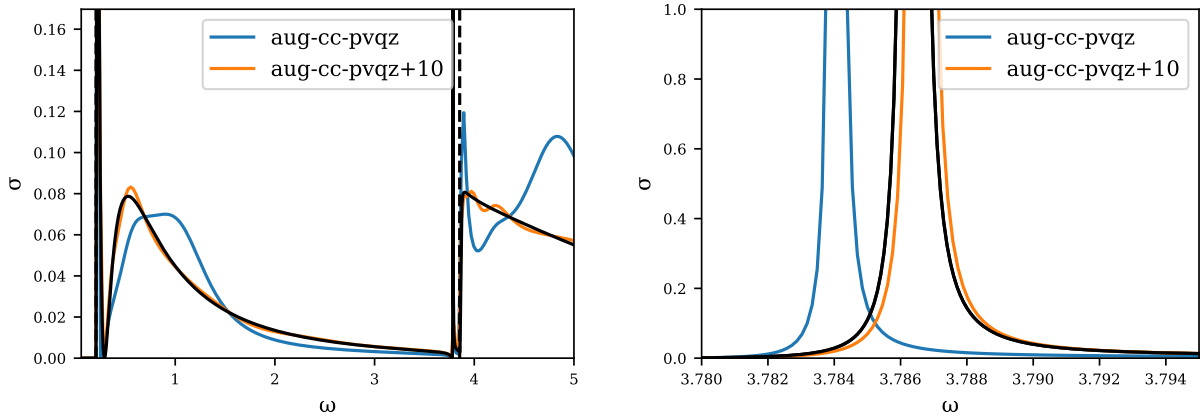


Figure 3: Photoionization of Beryllium (left), with zoom on the 1s→2p resonance (right).

almost converged at the aug-ccpvdz level. In particular, we find that moving from *aug* to *d-aug* basis sets turns out to be much more efficient, convergence-wise, than increasing the zeta label of the basis. This confirms again that the relevant components lies in the asymptotic part of the wave-function, supported by the delocalized atomic orbitals.

### 3.3 Polar molecule

We test the method on the strongly polarized LiH molecule. The strong dipole moment makes it hard for the method to converge, especially after the second ionization. Spurious oscillations after the peaks appear, which are consistent with what has been observed using approximate boundary conditions in radial methods [15]. However, we remark that these difficulties do not hinder the capture of both ionization thresholds.

### 3.4 Charged systems

We use $Li^+$ as a benchmark in this case. As any other charged systems, ions have a long-range total potential decaying in $1/r$. In such a case, the asymptotic form of the $\delta\psi$ is modified from a plane wave to a

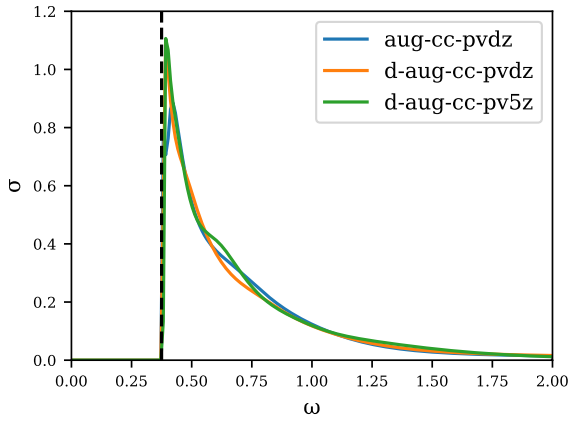


Figure 4: H2

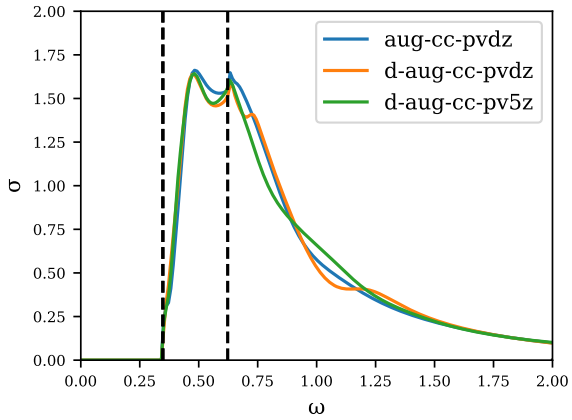


Figure 5: CH4

Coulomb wave [15, Appendix]. Therefore, the functions $\delta\phi$ become much more delocalized, and our method is inadequate.

Accordingly, there are strong oscillations after the ionization threshold, which disappear very slowly when increasing the basis set size; this is consistent with Figure 5 of [15]. For this example, the coarse integration grids we used before were not sufficient to resolve the fine oscillations, and we used a Gauss-Chebyshev grid with 100 points in the radial direction produced by PySCF.

# 4 Conclusion

We have presented a new method to compute photoionization spectra for TDDFT with semilocal exchange-correlation functionals in gaussian basis sets, and tested it on atoms and small molecules. The method appears to be very efficient on atoms and nonpolar molecules; it struggles on polar molecules and charged systems.

We note the following possible improvements to our methodology

- For simplicity, we used standard Dunning basis sets, with exchange-correlation integration grids.

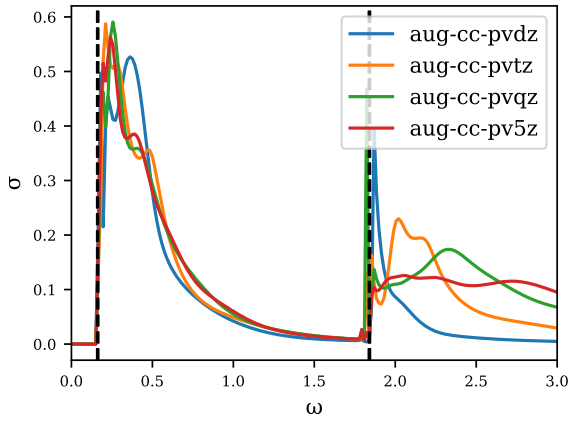


Figure 6: LiH

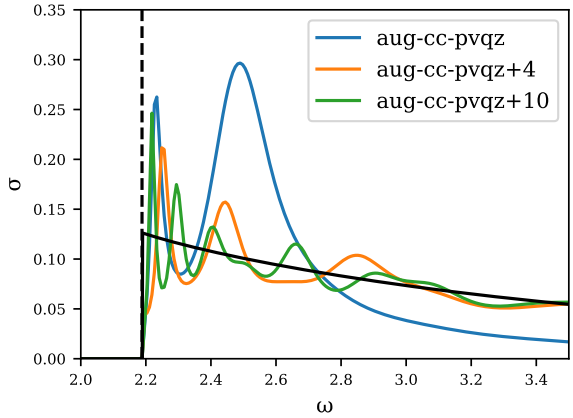


Figure 7: $Li^+$

Both of these were designed for a different problem (converging ground states orbitals and exchange-correlation integrals) than the one addressed here, and it is likely that computational efficiency can be significantly improved by tailoring these to our problem rather than using off-the-shelf technology.

- The current methodology scales formally as the fourth power of the number of electrons, with the possibility of cubic scaling at the cost of a higher prefactor. It should be possible to reduce this scaling even further using techniques like the resolution of the identity.

- Although we tested our scheme on semilocal density functionals, it is in theory straightforwardly adaptable to hybrid functionals. However, since the Sternheimer equation is effectively long-range in these cases [15], we expect to face the same difficulties as we did in the ionic case. An efficient treatment of the Coulomb potential is, as far as we know, an open problem in the non-radial case. A partial solution could be to truncate artificially the potential; this would yield better basis set convergence and eliminate the oscillations, at the price of a regularization of the problem (particularly important near ionization thresholds).

- We only explored linear response TDDFT in the frequency domain; it would be interesting to generalize this methodology to the non-perturbative TDDFT equations in the time domain. Recent progress has

been made in this direction in [10], using a similar decoupling between the kinetic and potential operators.

Finally, we note that we have focused here on atoms and small molecules. Experience suggests that it might be harder to converge photoionization spectra of small molecules than of large systems, because the relatively fine features computed here average out over a molecule, and because the basis sets used for larger molecules cover a larger region of space. Exploring this further is an interesting topic for future research.

## Acknowledgments

We are grateful to Karno Schwinn and Julien Toulouse for the reference data on atoms and ions.

## Appendix: matrix elements of the Helmholtz kernel in Gaussian basis sets

Our goal is the computation of integrals of the form

$$I = \langle g_1, G_0(\omega + i0^+) g_2 \rangle = -\frac{1}{2\pi} \int_{\mathbb{R}^6} g_1(\mathbf{r}) g_2(\mathbf{r}') \frac{e^{-\lambda|\mathbf{r}-\mathbf{r}'|}}{|\mathbf{r}-\mathbf{r}'|}.$$

when $g_1$ and $g_2$ are gaussian-type orbitals, for complex values of $\lambda$. The case of interest in the present paper is $\lambda = -i\sqrt{2\omega}$ (as well as possible analytic continuations of this). This also includes pointwise values of $G_0(\omega + i0^+)g_2$ by taking for $g_1$ the limit of a zero-width gaussian. Explicit formulas have been obtained in the context of range-separated hybrids with Yukawa potentials [17, 18, 1]; we recall here the method of computation.

As is standard, it suffices to compute the integral for the primitive radial gaussians $g_1(\mathbf{r}) = e^{-\alpha|\mathbf{r}-\mathbf{R}_1|^2}$, $g_2(\mathbf{r}) = e^{-\beta|\mathbf{r}-\mathbf{R}_2|^2}$. Expressions for integrals involving higher angular momenta can be obtained by differentiating the integrals with respect to the centers $\mathbf{R}_1$ and $\mathbf{R}_2$.

We use the integral representation:

$$\frac{e^{-\lambda x}}{x} = \sqrt{\frac{2}{\pi}} \int_0^\infty dt\, e^{-\frac{1}{2}(x^2 t^2 + \frac{\lambda^2}{t^2})}$$

and relatively straightforward but tedious changes of variables to obtain

$$I = -\frac{1}{2} \left(\frac{\pi}{\alpha}\right)^{3/2} \left(\frac{\pi}{\beta}\right)^{3/2} \frac{e^{-a^2 r^2}}{r} \left[ \operatorname{erfcx}\left(\frac{\lambda}{2a} + ar\right) - \operatorname{erfcx}\left(\frac{\lambda}{2a} - ar\right) \right]$$

with $a = \sqrt{\alpha\beta/(\alpha+\beta)}$ the combined Gaussian exponent, $r = |\mathbf{R}_t - \mathbf{R}_s|$ and where erfcx denotes the scaled complementary error function: $\operatorname{erfcx}(z) = e^{z^2}\operatorname{erfc}(z)$.

The computation of derivatives requires special care for numerical stability. We refer to [18] for a discussion of the issues and robust methods. We have implemented a similar method to that of [18] and generalized it to complex values of $\lambda$. Since we have found the method of [12, 2] to be very fast for the computation of error functions, we found that some of the complexity caused by the avoidance of these computations in [18] were not needed, and we use a slightly simplified implementation, using an upward recurrence relation (s1 in [18]) for large values of $ar$, and a Taylor expansion in $ar$ (s3 in [18]) for small values.

## References

[1] Yoshinobu Akinaga and Seiichiro Ten-no. Range-separation by the yukawa potential in long-range corrected density functional theory with gaussian-type basis functions. *Chemical Physics Letters*, 462(4-6):348–351, 2008.

[2] Mohammad Al Azah and Simon N Chandler-Wilde. Computation of the complex error function using modified trapezoidal rules. *SIAM Journal on Numerical Analysis*, 59(5):2346–2367, 2021.

[3] Jeff Bezanson, Alan Edelman, Stefan Karpinski, and Viral B Shah. Julia: A fresh approach to numerical computing. *SIAM review*, 59(1):65–98, 2017.

[4] Mark E Casida. Time-dependent density functional response theory for molecules. In *Recent Advances In Density Functional Methods: (Part I)*, pages 155–192. World Scientific, 1995.

[5] Alessandro Cerioni, Luigi Genovese, Ivan Duchemin, and Thierry Deutsch. Accurate complex scaling of three dimensional numerical potentials. *The Journal of chemical physics*, 138(20):204111, 2013.

[6] Emanuele Coccia, Roland Assaraf, Eleonora Luppi, and Julien Toulouse. Ab initio lifetime correction to scattering states for time-dependent electronic-structure calculations with incomplete basis sets. *The Journal of Chemical Physics*, 147(1):014106, 2017.

[7] Ivan Duchemin, Luigi Genovese, Eloïse Letournel, Antoine Levitt, and Simon Ruget. Efficient extraction of resonant states in systems with defects. *Journal of Computational Physics*, 477:111928, 2023.

[8] Thom H. Dunning. Gaussian basis sets for use in correlated molecular calculations. i. the atoms boron through neon and hydrogen. *J. Chem. Phys.*, 90:1007–1023, 1989.

[9] Mi-Song Dupuy and Antoine Levitt. Finite-size effects in response functions of molecular systems. *The SMAI Journal of computational mathematics*, 8:273–294, 2022.

[10] Jason Kaye, Alex Barnett, Leslie Greengard, Umberto De Giovannini, and Angel Rubio. Eliminating artificial boundary conditions in time-dependent density functional theory using fourier contour deformation. *arXiv preprint arXiv:2209.11027*, 2022.

[11] Rick A. Kendall, Thom H. Dunning, and Robert J. Harrison. Electron affinities of the first-row atoms revisited. systematic basis sets and wave functions. *J. Chem. Phys.*, 96:6796–6806, 1992.

[12] Pascal Molin. Multi-precision computation of the complex error function. working paper or preprint, March 2011.

[13] JG Muga, JP Palao, B Navarro, and IL Egusquiza. Complex absorbing potentials. *Physics Reports*, 395(6):357–426, 2004.

[14] Benjamin P Pritchard, Doaa Altarawy, Brett Didier, Tara D Gibson, and Theresa L Windus. New basis set exchange: An open, up-to-date resource for the molecular sciences community. *Journal of chemical information and modeling*, 59(11):4814–4820, 2019.

[15] Karno Schwinn, Felipe Zapata, Antoine Levitt, Eric Cancès, Eleonora Luppi, and Julien Toulouse. Photoionization and core resonances from range-separated density-functional theory: General formalism and example of the beryllium atom. *The Journal of Chemical Physics*, 2022.

[16] Qiming Sun, Xing Zhang, Samragni Banerjee, Peng Bao, Marc Barbry, Nick S Blunt, Nikolay A Bogdanov, George H Booth, Jia Chen, Zhi-Hao Cui, et al. Recent developments in the pyscf program package. *The Journal of chemical physics*, 153(2):024109, 2020.

[17] Seiichiro Ten-no. Initiation of explicitly correlated slater-type geminal theory. *Chemical Physics Letters*, 398(1-3):56–61, 2004.

[18] Seiichiro Ten-no. New implementation of second-order møller-plesset perturbation theory with an analytic slater-type geminal. *The Journal of chemical physics*, 126(1):014108, 2007.

[19] Bruno Nunes Cabral Tenorio, Sonia Coriani, Alexandre Braga Rocha, and Marco Antonio Chaer Nascimento. Molecular photoionization and photodetachment cross sections based on $l^2$ basis sets: Theory and selected examples. In *Advances in Methods and Applications of Quantum Systems in Chemistry, Physics, and Biology*, pages 151–179. Springer, 2021.